

COMPUTACIONAL ANALYSIS ON STRATIFIED TWO-PHASE OIL/WATER CO-CURRENT FLOW IN HORIZONTAL PIPES

M. Febres, mijail_febres@aluno.puc-rio.br

A. O. Nieckele, nieckele@puc-rio.br

Department of Mechanical Engineering, Pontificia Universidade Católica de Rio de Janeiro, PUC-Rio
Rua Marquês de São Vicente 225, Gávea - Rio de Janeiro, RJ - Brasil - 22453-900.

Abstract. *Stratified two-phase oil/water co-current flow in a horizontal pipeline can be often found in the petroleum industry. The correct prediction of the pressure drop is crucial for projects viability. At the present work, the flow was numerically obtained using commercial CFD package FLUENT 6.3, which is based on the finite volume method. The interface modeling was based on the VOF method, in which the relative amount of the fluids in each control volume is described by a variable, denominated here as volume fraction. Once the distribution of this quantity is known, it is possible to construct the interface, when needed. The turbulence model selected was the κ - ω SST model. The statistically steady state solution was analyzed and results of pressure drop, interface height and the axial velocity profiles were compared with experimental data.*

Keywords: *Two-Phase Flow, Stratified, Horizontal Pipeline, VOF.*

1. INTRODUCTION

The worldwide constantly raising demand of fuel for industry and higher quality standards for petroleum processing and transport equipment design has made the numerical prediction of multiphase flow inside pipelines, an important tool to reduce costs in comparison with expensive and sometimes not attainable experimental procedures.

In petroleum industry, during transport in pipelines, water and sometimes other phases and/or substances may flow along with oil, and depending on the phases superficial velocities it is possible to see the occurrence of several multiphase flow patterns, such as Smooth Stratified, Wavy Stratified, Elongated Bubble, Slug, Annular, Chaotic, etc.

For each of these flow patterns, it is desired to determine the individual hydrodynamic characteristics, such as pressure drop (among others) which is an important parameter for equipment and pipe design.

Among all these patterns, Stratified Two-phase Oil-Water flow is one of the most common patterns during operation in Petroleum processing facilities, and is main subject of this paper. Water, sometimes present in pipelines in water cuts above 60%, where operation is still economical, flows below the oil because of its higher density and produces gravity separation and hence a stratification of both phases under certain superficial velocity conditions.

There are many attempts to model two-phase stratified flow in literature, one of the most known treatments is the one of Taitel and Dukler (1976), based on a momentum balance on each phase, and more recently Newton and Behnia (2000) who developed, as an extension of the work of Issa (1988), a model to predict pressure drop and hold-up for turbulent two-phase smooth-stratified two-phase flow. Meknassi *et al.* (2000) proposed another model, on which, the interfacial interaction was introduced based upon experimental data on a bipolar coordinate system. Biderg (2002), developed an algebraic model to solve pressure drop and hold-up for two-phase laminar stratified pipe flow. Later on, in 2007, Biderg solved an algebraic model to predict two-phase turbulent stratified pipe flow. He was able to reproduce the effect of interfacial waves, obtaining good agreement between the model results and experimental data.

One of the first attempts to model stratified flow in 3D was presented by Mouza *et al.* (2001), who using a commercial code, simulated air and water in separated grids and prescribed the conditions on the interface of one phase grid, and exchange the information between the two grids until obtaining convergence. Ghorai *et al.* (2006) also simulated a two-phase stratified air-water flow with a commercial code, but they treated the interface as a moving rough wall. More recently, Vallée *et al.* (2008), also using a commercial code, predicted air-water wavy-stratified and slug flow in a square pipe and compare their results to experimental data.

Angeli and Hewitt (2000) studied, experimentally, the flow structure occurring during the flow of oil and water on two 0.0254 m tubes, one of steel and other of acrylic, and made comparisons between visual observations and probes data. Elseth (2002) published detailed velocity and turbulent LDA measurements data of a stratified horizontal oil-water flow. These data has been used by several authors to compare with numerical predictions of the flow. Hapanowicz (2008), tried, experimentally, to establish a relationship between the slip and the real (in situ) volume fraction for oil-water mixtures.

Elseth *et al.* (2000) presented a numerical comparison of the flow obtained with FLUENT, with the experimental data of a stratified horizontal oil-water flow. The agreement between the predictions and experimental data was only qualitative, since the influence of the interface in the flow was not correctly taken into account. Hui Gao *et al.* (2003) and Kumara *et al.* (2008) employed a 3-D formulation, with a modified VOF model, in order to predict a smooth transition between phases, to numerically reproduce Elseth's experimental data, and reasonable agreement was obtained.

In the present work, the commercial CFD software FLUENT™ was employed to solve numerically the oil-water two-phase stratified flow. The interface was determined using the standard VOF (volume of fluid) model (Hirt and Nichols, 1981). Turbulence was taken in account with the $\kappa\omega$ SST model (Menter, 1994). The surface tension was modeled using the built-in Continuum Surface Force (CSF) model (Brackbill *et al.*, 1992) in FLUENT™. The mean velocity profile, volume fraction, as well as turbulent quantities were compared with the experimental data of Elseth (2002).

2. MATHEMATICAL MODELING

To determine the two-phase stratified flow field inside a horizontal pipeline, the VOF (volume of fluid) model (Hirt and Nichols, 1981) was selected. The VOF model is capable of modeling two or more immiscible fluids by solving one single set of equations, for conservation of mass and conservation of momentum. This method is based on use of a variable called “volume fraction”, α_i , which can tell where each of the phases can be found. All fields for variables and properties are shared by all the phases, and they represent average values. Properties and variables on each cell are entirely representative of one phase or a mixture of the phases depending on the value of volume fraction, which are defined as follows: $\alpha_i = 0$ if the cell does not contain fluid “*i*”, $\alpha_i = 1$ if the cell is full of fluid “*i*” and $0 < \alpha_i < 1$ if the cell contains the interface between the phases. For each new phase introduced in the problem, a new variable for the volume fraction is created, and in each cell, the sum of all volume fractions is equal to 1. At the present problem, there is only two phases present, thus, $n=2$.

$$\sum_{i=1}^n \alpha_i = 1 \quad (1)$$

Properties, like density (ρ) and viscosity (μ), which appear in transport equations, are evaluated by taking in account the amount of each phase in the cell, as follows:

$$\rho = \sum_{i=1}^n \alpha_i \rho_i \quad ; \quad \mu = \sum_{i=1}^n \alpha_i \mu_i \quad (2)$$

The interface tracking is determined by assuming a material derivative of the interface equal to zero for a referential on the interface, thus

$$\frac{\partial \alpha_i}{\partial t} + \bar{u} \cdot \nabla \alpha_i = 0 \quad (3)$$

where \bar{u} is the time average velocity vector.

The Reynolds average continuity and momentum equation can be written as

$$\frac{\partial}{\partial t} (\rho \bar{u}) + \nabla \cdot (\rho \bar{u}) = 0 \quad (4)$$

$$\frac{\partial}{\partial t} (\rho \bar{u}) + \nabla \cdot (\rho \bar{u} \bar{u}) = -\nabla p + \rho \bar{g} + \nabla \cdot [(\mu + \mu_t) 2 \underline{\underline{S}}] + \rho \bar{g} + \bar{F} \quad (5)$$

where p is the pressure, \bar{g} is the gravity acceleration vector, μ and μ_t are the molecular and turbulent viscosity, $\underline{\underline{S}}$ is the mean rate of strain tensor

$$\underline{\underline{S}} = \frac{1}{2} \left(\nabla \bar{u} + \nabla \bar{u}^T \right) \quad (6)$$

and \bar{F} is an external force which takes in account the effects of surface tension (σ_{ij}) of two phases. FLUENT™ uses CSF (Continuum Surface Force) developed by Brackbill *et al.* (1992), which is based on the curvature R_i of the interface, and in the volume fraction gradient in cells that contains the interface as

$$\bar{F} = \sigma_{ij} \frac{\rho R_i \nabla \alpha_i}{(\rho_i + \rho_j)/2} \quad ; \quad R_i = \nabla \cdot \bar{\hat{n}}_i \quad ; \quad \bar{\hat{n}}_i = \frac{\bar{n}_i}{|\bar{n}_i|} \quad ; \quad \bar{n}_i = \nabla \alpha_i \quad (7)$$

The shear-stress transport (SST) κ - ω model was employed to model turbulence. This model was developed by Menter et al. (1994), it consists on an accurate formulation of the standard κ - ω formulation in the near-wall region and the κ - ε model in the far field. The κ - ε model is converted into a κ - ω formulation, by multiplying each equation by a blending function and then added together. Those blending functions are design to be one in the near-wall region to activate the κ - ω model and zero away from the surface, which activates the κ - ε model. The turbulent viscosity is defined as

$$\mu_t = \frac{1}{f_\mu} \frac{\rho \kappa}{\omega} \quad ; \quad f_\mu = \max\left(\frac{1}{\alpha^*}, \frac{S F_2}{a_1 \omega}\right) \quad ; \quad S = \sqrt{2 S_{ij} S_{ij}} \quad (8)$$

where S is the modulus of the strain-rate, α^* is a coefficient that damps the turbulent viscosity causing a low-Reynolds-number correction, and F_2 is a blending function

$$\alpha^* = \left(\frac{\alpha_o^* + \text{Re}_t / R_\kappa}{1 + \text{Re}_t / R_\kappa}\right) \quad ; \quad \text{Re}_t = \frac{\rho \kappa}{\mu \omega} \quad (9)$$

$$F_2 = \tanh(\Phi_2^2) \quad ; \quad \Phi_2 = \max\left[2 \frac{\sqrt{\kappa}}{0.09 \omega y}, \frac{500 \mu}{\rho y^2 \omega}\right] \quad (10)$$

y is the distance to the next surface. The empirical constants are: $a_1 = 0.31$; $\alpha_o^* = 0.072/3$; $R_\kappa = 6$.

The turbulence kinetic energy, κ , and specific dissipation rate, ω , are obtained from the following transport equation

$$\frac{\partial}{\partial t}(\rho \kappa) + \frac{\partial}{\partial x_i}(\rho \kappa u_i) = \frac{\partial}{\partial x_j} \left[\left(\mu + \frac{\mu_t}{\sigma_\kappa} \right) \frac{\partial \kappa}{\partial x_j} \right] + G_\kappa - Y_\kappa \quad (11)$$

$$\frac{\partial}{\partial t}(\rho \omega) + \frac{\partial}{\partial x_i}(\rho \omega u_i) = \frac{\partial}{\partial x_j} \left[\left(\mu + \frac{\mu_t}{\sigma_\omega} \right) \frac{\partial \omega}{\partial x_j} \right] + G_\omega - Y_\omega + D_\omega \quad (12)$$

where σ_κ and σ_ω are the turbulent Prandtl numbers:

$$\sigma_\kappa = \frac{1}{\frac{F_1}{\sigma_{\kappa,1}} + \frac{(1-F_1)}{\sigma_{\kappa,2}}} \quad ; \quad \sigma_\omega = \frac{1}{\frac{F_1}{\sigma_{\omega,1}} + \frac{(1-F_1)}{\sigma_{\omega,2}}} \quad \text{where} \quad F_1 = \tanh(\Phi_1^4) \quad (13)$$

and G_κ and G_ω represent the generation of κ and ω due to mean velocity gradients, Y_κ and Y_ω , represents dissipation of κ and ω due to turbulence and D_ω is the cross-diffusion term, given by

$$G_\kappa = \min(\mu_t S^2; 10 \rho \beta^* \kappa \omega) \quad ; \quad G_\omega = \alpha \rho S^2 \quad ; \quad Y_\kappa = \rho \beta^* \kappa \omega \quad ; \quad Y_\omega = \rho \beta \omega^2 \quad (14)$$

$$D_\omega = (1 - F_1) \sigma_{\omega 2} D_\omega^* \quad ; \quad D_\omega^* = \rho \frac{2}{\omega} \frac{\partial \kappa}{\partial x_j} \frac{\partial \omega}{\partial x_j} \quad (15)$$

The remaining auxiliary parameters are

$$\Phi_1 = \min \left[\max \left(\frac{\sqrt{\kappa}}{0.09 \omega y}, \frac{500 \mu}{\rho y^2 \omega} \right), \frac{4 \rho \kappa}{\sigma_{\omega,2} D_\omega^+ y^2} \right] \quad ; \quad D_\omega^+ = \max \left(\frac{D_\omega^*}{\sigma_{\omega 2}}; 10^{-10} \right) \quad (16)$$

$$\beta^* = 0.09 \frac{4/15 + (\text{Re}_t / R_\beta)^4}{1 + (\text{Re}_t / R_\beta)^4} \quad ; \quad \alpha = \frac{\alpha_\infty}{\alpha^*} \left(\frac{1/9 + \text{Re}_t / R_\omega}{1 + \text{Re}_t / R_\omega} \right) \quad (17)$$

$$\alpha_{\infty} = \left[\frac{0.075}{\beta_{\infty}^*} - \frac{\kappa^2}{\sigma_{\omega,1} \sqrt{\beta_{\infty}^*}} \right] F_1 + \left[\frac{0.0828}{\beta_{\infty}^*} - \frac{\kappa^2}{\sigma_{\omega,2} \sqrt{\beta_{\infty}^*}} \right] (1 - F_1) \quad (18)$$

$$\beta = 0.075 \quad ; \quad F_1 + 0.0828 (1 - F_1) \quad (19)$$

Additional empirical constants are: $\sigma_{\kappa,1} = 1.176$; $\sigma_{\omega,1} = 2$; $\sigma_{\kappa,2} = 1.0$; $\sigma_{\omega,2} = 1.168$; $\alpha_o^* = 0.072/3$; $R_{\beta} = 8$; $R_{\omega} = 2.95$, $\beta_{\infty}^* = 0.09$.

3. NUMERICAL METHOD

To allow comparison with the experimental data of Elseth (2002), it was considered the same pipeline, with diameter $D = 0.05575$ m and length $L = 5$ m, approximately equal to $100 D$, in order to guarantee that fully developed flow would be attained.

The computational domain was made according to the experimental data of Elseth (2002). GAMBIT™ was employed to generate a mesh with 4.13×10^6 cells, with 1652 cells in the cross section and 250 cells in the axial direction, where the grid size was increased gradually in the direction to the outlet. The inlet section as shown in Fig. 1 was divided into 2 sections, one for oil inlet above the one for water, with 826 cells for each one.

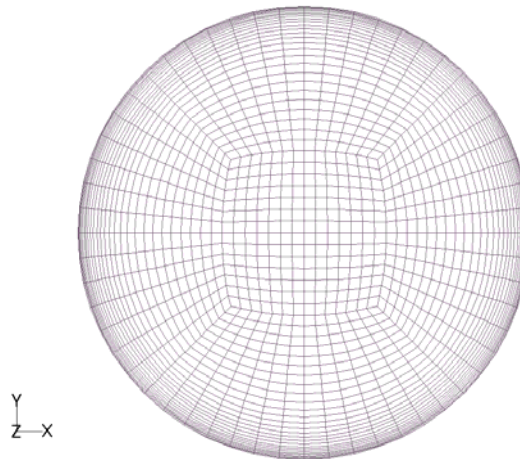


Figure 1. Cross-section of the pipe grid

The conservation equations, discretized by the Finite Volume method, were solved by FLUENT™. To solve the velocity-pressure coupling, the PISO algorithm was selected, the scheme of discretization for pressure was PRESTO, geometric reconstruction for the volume fraction, and the QUICK scheme was used for momentum, turbulent kinetic energy and specific dissipation rate. Non-iterative time advancement was employed to advance in time. Residual tolerance was set as 0.0001. Each case was simulated until stabilization for velocity and pressure was obtained.

4. RESULTS

The velocity, pressure and volume fraction fields were obtained considering at both inlets (for oil and water), uniform velocity profiles, and constant pressure at the outlet, according to the experimental data available. Turbulence parameters were prescribed as follows: turbulence intensity of 5% and the corresponding hydraulic diameter equal to the pipeline diameter. Non-slip condition was prescribed at the wall. The computational solution was initialized with a volume fraction of 0.5 for all cases, and a velocity field according to the inlet boundary. The specified fluid properties for oil and water are listed in Table 1.

Table 1. Fluids properties.

Fluid	ρ (kg/m ³)	μ (Pa-s)	σ (N/m)
Oil	790	0.00164	0.043
Water	1000	0.00102	

The mixture velocity U_m is defined as the ratio of the volumetric flow rate Q to cross section area A ($U_m = Q/A$) and it is equal the sum of the superficial oil and water velocities, U_{so} and U_{sw} , respectively ($U_m = Q/A = U_{so} + U_{sw}$). The water cut is the ratio of the water and total flow rate, $C_w = Q_w/Q = U_{sw}/U_m$.

The VOF model is adequate to predict sharp interfaces, therefore, among the several cases measured by Elseth (2002), only the ones that present an approximately sharp interface can be predicted with such a model. Therefore, based on the available experimental data of Elseth (2002), two cases were selected to be investigated, corresponding to a mixture velocity U_m of 0.68 m/s (Case 1) and 1.02 m/s (Case 2), both with water cut C_w equal to 0.5. Figure 2 presents photographs from Elseth (2002) for the two cases. For Case 1, the volume fraction (or holdup) is also shown, while for Case 2, besides the holdup, velocity and turbulent quantities profiles were also superimposed to the flow picture. It can be clearly seen that for both cases the interface thickness is of the order of 20%-30% of the pipe diameter.

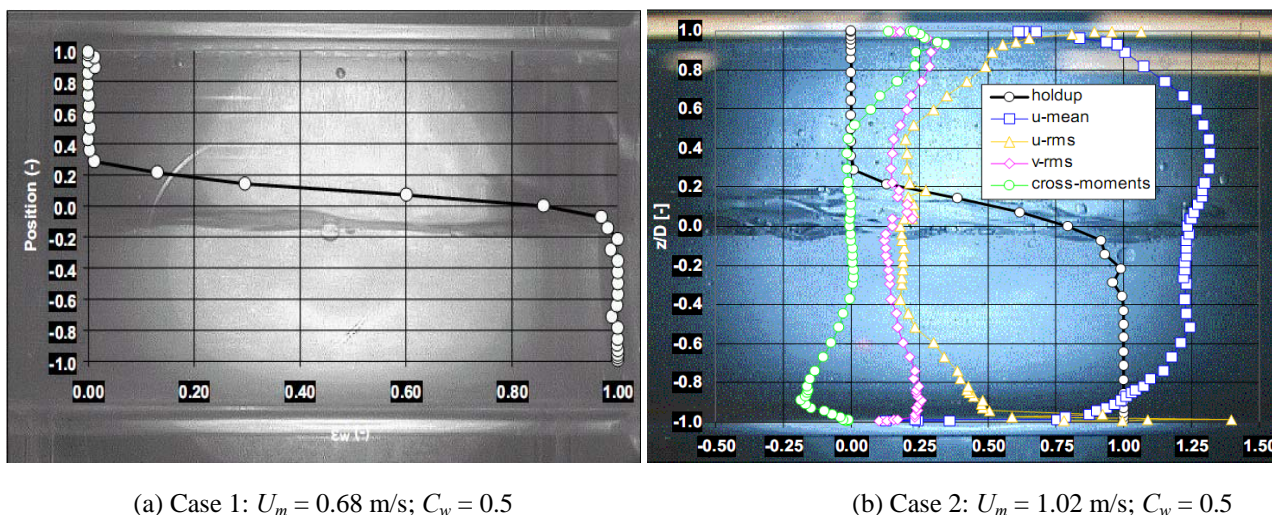


Figure 2. Test section Photograph of Case 1 and Case 2, Elseth (2002).

Figures 3 and 4 illustrates a comparison of the present numerical results with the experimental data of Elseth (2002), for the axial velocities profiles and volume fraction, along a vertical line at the center of the pipe, at an axial position equal to 4 m ($72 D$), where it was observed that fully developed flow conditions had been attained. Figure 3 corresponds to Case 1, while Fig. 4 corresponds to Case 2.

Figure 3a illustrates the axial velocity profile, while Fig. 3b shows the volume fraction for Case 1. As it can be seen from Fig. 3a, the agreement between the water velocity profile with the experimental data is reasonable, however the inflexion point at the interface was not captured by the VOF model. As a consequence the faster oil flow was not accurately predicted. By examining the volume fraction distribution in Fig. 3b, it can be observed that qualitatively the volume fraction distribution is correct, however while VOF predicts a sharp interface, actually there is a mixture region, as it was shown in the photograph at Fig. 2a. Further, it can also be noticed the presence of some waves at the interface, and this phenomenon could not be reproduced numerically.

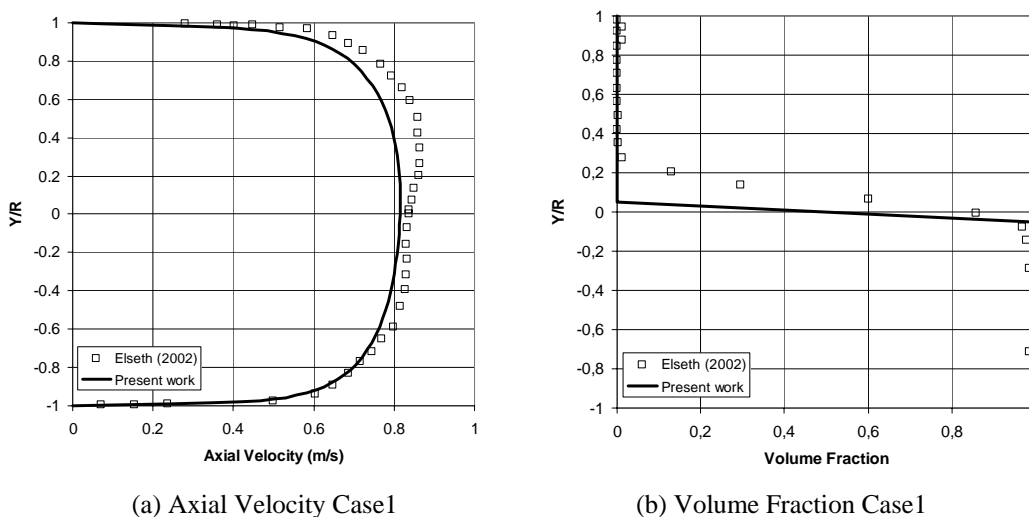


Figure 3. Comparison between experimental data vs. Numerical simulation. Case 1: $U_m = 0.68$ m/s; $C_w = 0.5$

The same type of results is shown in Fig. 4 for Case 2, which corresponds to a higher mixture velocity. Once again the prediction of the water velocity profile is reasonable and the holdup distribution is qualitatively satisfactory. Note however, that, as the mixture velocity increases, the agreement between the results deteriorates, since the interface region increases.

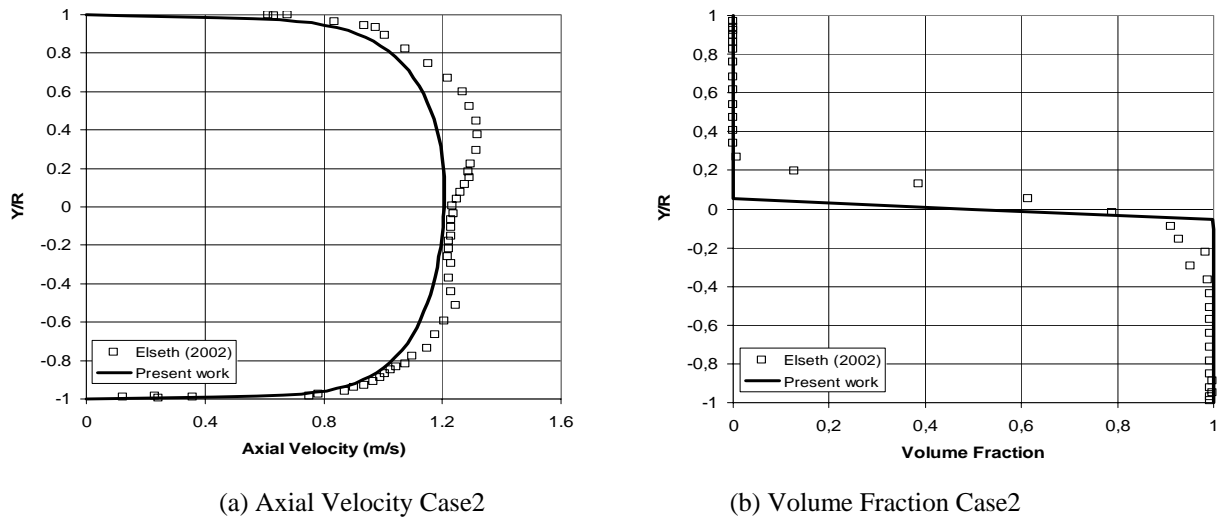


Figure 4. Comparison between experimental data vs. Numerical simulation. Case 2: $U_m = 1.02$ m/s; $C_w = 0.5$

Table 3 presents the experimental and numerical maximum velocity, where it can be seen that although the numerical model underpredicted the maximum velocity, the error in relation to the experimental data is equal to only 5.4 % and 8.4 % for each case.

Table 3. Maximum Velocity.

Case	U_{max} (Present Work)	U_{max} (Elseth 2002)	Error %
Case1	0.816	0.863	5.4
Case2	1.207	1.318	8.4

Experimental data suggests that for water cuts of 50%, the maximum velocity should be in the lighter phase (oil). Indeed, for both cases, the predicted maximum oil velocity is larger than the maximum water velocity, but the difference obtained is quite small. We might say that numerical velocity profiles are not representing the bulk velocity, but if we look closely, it is possible that a velocity profile, only in a vertical central line, is not enough to show the bulk velocity, because we do not know how velocity is acting in other sections of the pipe. Elseth (2002) mentions some differences in the data measured depending on the technique employed. The flow rate obtained by integrating the velocity profile measured with LDA (Laser Doppler Anemometry) was compared with the flow meter readings. The results suggested that LDA velocity profile shows higher values, because the Plexiglass section narrows down from 0.0558m to 0.0553m in its internal diameter and its entry has a smooth transition to reduce the 0.0563m diameter of the steel section on the pipe to 0.0558m diameter of the test section. This could be one of the reasons of the difference between numerical maximum and experimental velocity.

Another interesting way to examine the velocity profile is through the dimensionless velocity and position based on the friction velocity u^*

$$u^+ = \frac{u}{u^*} \quad ; \quad y^+ = \frac{\rho u^* y}{\mu} \quad ; \quad u^* = \sqrt{\tau_w / \rho} \quad (20)$$

where the mixture properties are given by Eq. (2) and $\overline{\tau_w}$ is the average shear stress at the pipeline wall. Figure 5 presents for Case1 and Case2, numerical and experimental dimensionless velocity as a function of the dimensionless distance to the wall. Oil data is presented in black, while water data in blue. In the same figures, the universal linear profile corresponding to the sub-layer and logarithmic profile of the turbulent core are also included. Figs. 5a and 5b. show good agreement between the numerical and experimental data in the central part of the pipe, with the logarithmic behavior, since the wall law was employed in the simulations. Note however that those profiles present a slight different

inclination than the universal law. Indeed, there are several discussions in the literature that argue that the velocity slope should not be given by the Von Kármán constant. In the near-wall there are some data some dispersion, which might be produced by the few values and the difficulty to obtain them using LDA near the wall. As already observed in Figs. 3 and 4, the agreement with the water data is quite superior to the oil data.

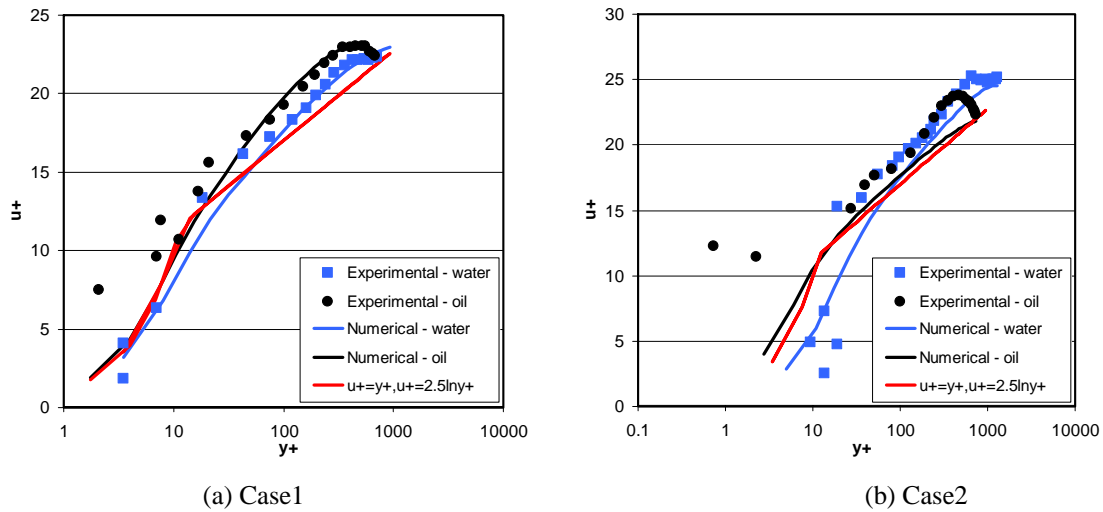


Figure 5. Comparison between experimental data vs. numerical simulation for $u^+ y^+$.

Turbulent quantities like turbulent intensity and cross-moments are shown in Figs. 6 and 7. Turbulent intensity was calculated according to Elseth (2002) with the following expression:

$$T. I.(%) = \frac{rms(u'u')}{u} 100\% \tag{21}$$

where $rms(u'u')$ and the cross momentum $\overline{u'v'}$ were obtained from the mean axial velocity profile in accordance with the $\kappa-\omega$ turbulence model as,

$$rms(u'u') = \sqrt{2 \frac{\mu}{\rho} \frac{\partial u}{\partial x} - \frac{2}{3} \kappa} ; \quad \overline{u'v'} = -\frac{\mu}{\rho} \left(\frac{\partial u}{\partial y} + \frac{\partial v}{\partial x} \right) \tag{22}$$

Figure 6 shows for both cases a reasonable agreement, with the same level of turbulence in almost the whole domain. It can be seen again, that in the interface region, the model fails to capture correctly the reduction of the turbulence intensity, which certainly influences the velocity reduction at the same region. The numerical model was also not able of predicting the high levels of turbulence intensity, near the walls, as measured.

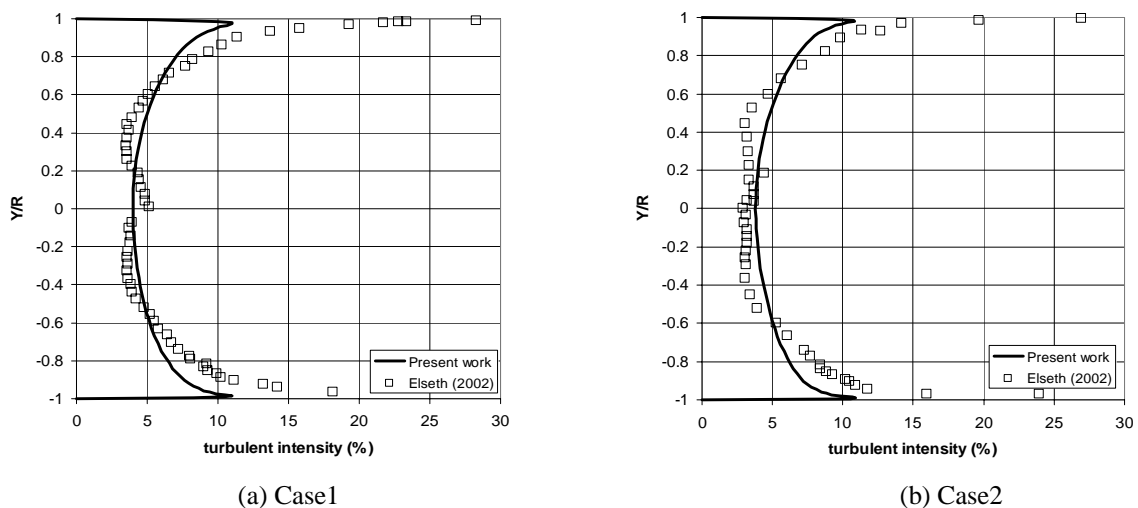


Figure 6. Comparison between experimental data vs. Numerical simulation for Turbulent Intensity.

The cross-momentum profiles are shown in Fig. 7. Here, it can be seen, approximately the same trend and order of magnitude of the numerical and experimental data. Analyzing the experimental data, once can observe that at the interface region, there is an interaction between the oil and water, and the cross momentum goes to zero. This behavior was not capture by the turbulence model, indicating that the turbulence model must also be adjusted in order to reduce the cross-momentum at the interface region.

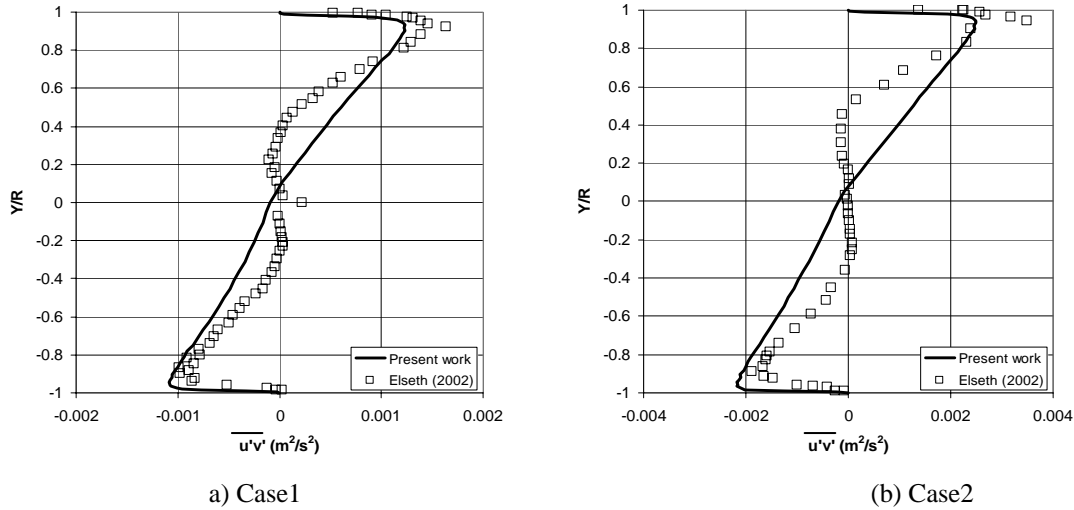


Figure 7. Comparison between experimental data vs. Numerical simulation for Cross Moments.

Pressure gradient can be calculated by employing an overall momentum balance as

$$-\frac{\partial p}{\partial x} = \frac{\overline{\tau_w}(S_o + S_w)}{A} = \frac{\tau_{ow}S_o + \tau_{ww}S_w}{A} ; \tau_{iw} = f_i \frac{\rho_i u_i^2}{2} \quad (23)$$

where τ_{iw} is the wall shear stress of each phase, and $\overline{\tau_w}$ is the average shear stress at the pipeline wall, A is the pipe cross section area equal to $A_w + A_o$ where A_i and S_i are the phase cross section area and wetted perimeter. From the solution field numerically obtained the pressure gradient was determined based on the average wall shear stress. To allow comparison with available literature correlation, the pressure gradient was also determined based on the friction factor correlation of Haaland (1983), which is as a function of the phase Reynolds number Re_i , hydraulic diameter D_{hi} and the pipe roughness e , which was here neglected.

$$f_i = \left(-3.6 \log_{10} \left(\frac{6.9}{Re_i} + \left(\frac{e/D_{hi}}{3.7} \right)^{1.1} \right) \right)^{-2} ; Re_i = \frac{\rho_i U_i D_{hi}}{\mu_i} ; D_{hi} = \frac{4 A_i}{S_i} \quad (24)$$

Those two values were compared with the experimental data of Elseth (2002) in Table 4. Note that the predicted value agrees quite well with the correlation, indicating that the presence of the mixture region is indeed the main cause of discrepancies between the results.

Table 4. Pressure Gradient.

Case	$-\frac{\partial p}{\partial x}$ (Pa/m) (Elseth 2002)	(Present Work)		(Overall momentum balance)	
		$-\frac{\partial p}{\partial x}$ (Pa/m)	Error %	$-\frac{\partial p}{\partial x}$ (Pa/m)	Error %
Case1	90.82	82.68	8.92	89.45	1.51
Case2	173.47	163.24	5.90	183.46	5.76

5. CONCLUSIONS

At the present work, oil and water horizontal stratified flow was numerically predicted with the κ - ω turbulence model, and the VOF model. The overall results were reasonable, with good agreement of the total pressure drop.

However, the predictions were not sufficiently accurate at the interface region. Therefore, from the results, we can say that standard VOF model should not be used when there is not a well defined interface between the phases. The presence of a mixture region reduces the velocity as well as turbulence, resulting on a velocity profile with a concavity, which could not be predicted.

On experimental observations, we can see some waves at the interface, which could also not be reproduced with VOF. As the mixture velocity increases, the mixture region also increases, with a large presence of bubbles, and this suggests that maybe the VOF method could be combined with a drift model to be able to reproduce the velocity profile at the interface.

6. ACKNOWLEDGEMENTS

The second author also thanks the Brazilian Research Council, CNPq, for the support awarded to this work.

7. REFERENCES

- Angeli p., Hewitt, g.f., 2000, "Flow structure in horizontal oil–water flow", *International Journal of Multiphase Flow* 26, 1117–1140.
- Brackbill J. U., Kothe D.B. and Zemach C., 1992, "A continuum method for modelling surface tension", *J. Comp. Phys.*, 100, pp. 335-354.
- Biderg, D., 2002, "Holdup And Pressure Drop In Two-Phase Laminar Stratified Pipe Flow", *Multiphase Science and Technology*, Vol. 14, No. 4, pp. 267-301.
- Biderg, D., 2007, "A Mathematical Model For Two-Phase Stratified Turbulent Duct Flow", *Multiphase Science and Technology*, Vol. 19, No. 1, pp. 1–48.
- Elseth G., 2002, "An Experimental Study of Oil / Water Flow in Horizontal Pipes", PhD Thesis, The Norwegian University of Science and Technology (NTNU).
- Elseth, G., Kvandal, H.K., Melaaen, M.C., 2000, "Measurement of velocity and phase fraction in stratified oil/water flow", *International Symposium on Multiphase Flow and Transport Phenomena*, Antalya, Turkey, pp. 206-210.
- Ghorai, s., Nigam K.D.P., 2006, "CFD modeling of flow profiles and interfacial phenomena in two-phase flow in pipes", *Chemical Engineering and Processing* 45 55–65.
- Haaland S.E., 1983, "Simple and Explicit Formulas for the Friction Factor in Turbulent PipeFlow", *Journal of Fluids Engineering* Vol.105.
- Hapanowicz j., 2008, "Slip between the phases in two-phase water–oil flow in a horizontal pipe", *International Journal of Multiphase Flow* 34 559–566.
- Hirt, C.W. and Nichols, B. D., 1981, "Volume of Fluid (VOF) Method for the Dynamics of Free Boundaries", *J. Comput. Phys.*, Vol. 39, pp. 201-225.
- Hui Gao, Han-Yang Gu, Lie-Jin Guo, 2003, "Numerical study of stratified oil–water two-phase turbulent flow in a horizontal tube", *International Journal of Heat and Mass Transfer* 46 749–754.
- Kumara, W.A.S. , Elseth, G., Halvorsen B.M., Melaaen, M.C., 2008, "Computational Study Of Stratified Two Phase Oil/Water Flow In Horizontal Pipes", 6th International Conference on Heat Transfer, Fluid Mechanics and Thermodynamics 30 June to 2 July 2008 Pretoria, South Africa.
- Meknassi, F., Benkirane, R., Line, A., Masbernat, L., 2000, "Numerical modeling of wavy stratified two-phase flow in pipes", *Chemical Engineering Science* 55 4681-4697.
- Menter, F. R., 1994, "Two-Equation Eddy-Viscosity Turbulence Models for Engineering Applications." *AIAA Journal*, 32(8):1598-1605.
- Mouza, A. A., Paras, S. V., Karabelas, A. J., 2001, "CFD code application to wavy stratified Gas-liquid flow", *Institution of Chemical Engineers Trans IChemE*, Vol 79, Part A.
- Newton, C. H., Behnia, M., 2000, "Numerical calculation of turbulent stratified gas–liquid pipe flows", *International Journal of Multiphase Flow* 26 327–337.
- Taitel, Y. and Dukler, A.E., 1976, "A model for predicting flow regime transitions in horizontal and near horizontal gas liquid flow. *AIChE J.* 22, pp. 47-55.
- Vallée, C., Höhne, T., Prasser, H.M., Sühnel, T, 2008, "Experimental investigation and CFD simulation of horizontal stratified two-phase flow phenomena", *Nuclear Engineering and Design* 238 637–646.
- Vlachos, N.A., Paras, S.V., Karabelas, A.J., 1999, "Prediction of holdup, axial pressure gradient and wall shear stress in wavy stratified and stratified/atomization gas/liquid flow", *International Journal of Multiphase Flow* 25, 365–376.

8. RESPONSIBILITY NOTICE

The authors are the only responsible for the printed material included in this paper.